2023

Estimating Battery Size Requirements for Tractor Electrification of Row-Crop Planting Operations

CheeTown Liew
University of Nebraska-Lincoln, cliew2@unl.edu

Andrew Donesky
University of Nebraska-Lincoln, adonesky2@huskers.unl.edu

Mark Freyhof
University of Nebraska-Lincoln, mfreyhof2@huskers.unl.edu

Ian Tempelmeyer
University of Nebraska-Lincoln, ian.tempelmeyer@gmail.com

Santosh Kumar Pitla
University of Nebraska-Lincoln, spitla2@unl.edu

ESTIMATING BATTERY SIZE REQUIREMENTS FOR TRACTOR ELECTRIFICATION OF ROW-CROP PLANTING OPERATIONS

Research

CheeTown Liew[1,*], Andrew Donesky[1], Mark Freyhof[1], Ian Tempelmeyer[1], Santosh Kumar Pitla[1]

[1] Department of Biological Systems Engineering, University of Nebraska, Lincoln, Nebraska, USA.
[*] Correspondence: cliew2@unl.edu

HIGHLIGHTS

- Calculate and compare engine power needed for row-crop planting from ASAE standards and reported CAN data.
- Estimate energy requirements and the equivalent electric battery's volume and mass for row-crop tractor.
- Discuss the feasibility for electrification of a fully electric row-crop tractor.

ABSTRACT. *Power sources such as batteries, used for both on-road and off-road vehicles, are advancing at a rapid pace. Electric batteries are becoming more power dense, thus allowing them to be used as a power source to replace previous diesel or gasoline-powered systems. Efforts are underway to transition off-road agricultural vehicles from Internal Combustion Engine (ICE) vehicles to electric vehicles (EVs); however, the energy requirements of typical agricultural field operations need to be fully understood before such a transition can occur. Theoretical prediction equations available in the American Society of Agricultural and Biological Engineers (ASABE) standards or the use of engine load data from a tractor's Controller Area Network (CAN) bus are two methods for determining the energy demands of implements on tractors. In this study, tractor CAN bus data was collected from multiple no-till corn planting operations to estimate the energy requirements of the planting operation in kWh. The estimated energy requirement was used to determine the equivalent physical mass and volume of a lithium-ion battery needed to power a hypothetical fully electric tractor for comparable planting operations. The estimated battery capacities using the worst-case field-use scenario in this study were 1117 kWh for operating a 16-row planter to plant 68 ha (168 acre) in a day at an average ground speed of 8.6 km h^{-1} (5.4 mph) for 14 hours, and 2658 kWh for operating a 48-row planter to plant 158 ha (391 acre) in a day at an average ground speed of 8.9 km h^{-1} (5.6 mph) for 15 hours. Given the current battery energy density requirements, the equivalent battery masses and volumes were found to be 5,319 kg and 3.33 m^3, 12,657 kg and 7.93 m^3, for 16-row planter and 48-row planter, respectively. These high kWh estimates needed to power future fully-electric tractor power units are based on worst-case scenarios that could be encountered in real field operations that use wide planters over long operating hours.*

Keywords. *Battery, Controller Area Network, Electric Vehicles, Electrification, No-till, Planting, Row-crop, Tractor.*

The push to use non-fossil-based energy sources has motivated many vehicle manufacturers, such as Tesla, to explore electric power as an environmentally sustainable alternative to gasoline or diesel power. For many off-road vehicle applications such as mining, construction, and agriculture, diesel is the dominant energy source; however, fully electric off-road vehicles are being explored (Caterpillar, 2022; Gaetjens, 2022; Hart, 2022; NHK World-Japan, 2023; Sensiba, 2022). The agricultural sector makes up a large portion of the off-road vehicle industry, where both low-power (less than 75 kW or 100 hp) and high-powered equipment (more than 75 kW or 100 hp) are required. Extensive efforts are underway to electrify lower-powered agricultural equipment with commercial examples such as the Kubota, Monarch, or Soletrac tractors (Kubota Corporation, 2022; Monarch Tractor, n.d.; Soletrac, n.d.). High-powered agricultural equipment for large-scale row-crop production has also seen electrification innovations. Some examples include John Deere's SESAM2 (Sustainable Energy Supply for Agricultural Machinery) electric tractor with a 1000kWh battery (Van Erkelens, 2022) and John Deere's GridCON tractor, operating with a tethered electric cable for a theoretically unlimited operational time (Van Hattum, 2019). New Holland's T4-Electric Power all-electric utility tractor has a peak power of 98 kW, or 120 hp, but with an undisclosed battery size (CNH Industrial, 2022). These prototypes of row-crop electric tractors have certain limitations; they either require a tethered power source or can only operate for a limited working time. (Rohrer, 2017). To further advance electrification efforts for both classes of agricultural equipment, it is necessary to calculate power and

Submitted for review on 3 February 2023 as manuscript number MS 15556; approved for publication as a Research Article by Associate Editor Dr. Sami Khanal and Community Editor Dr. Heping Zhu of the Machinery Systems Community of ASABE on 7 August 2023.

  ISSN 2769-3295 https://doi.org/10.13031/ja.15556

energy requirements for each specific agricultural operation to better understand the necessary energy demands that electric powered agricultural equipment would need to support.

Two methods could be used to calculate power and energy requirements for agricultural operations. The first is the use of American Society of Agricultural and Biological Engineers (ASABE) Standards, such as EP496.3 and D497.7 (ASABE Standards, 2020a,b). While these standards were created to help calculate specific power demands for agricultural operations such as planting, the tabulated data in the standards are based around equipment from at least four decades ago (ASABE Standards, 2020a,b). A second method is collecting built-in sensor data communicated over the Controller Area Network (CAN) bus to calculate real-time power demands. In addition to establishing communication among multiple electronic control units (ECUs), the CAN bus allows users to collect machine operation data without the need for external instrumentation and sensors, and is an essential component of modern off-road and agricultural machinery (Marx, 2015). The accuracy of the data generated from on-board sensors communicated over the CAN bus has been validated by researchers. Comparing fuel rate data obtained from the CAN bus with physical fuel rate measurements, it was found that CAN bus data is accurate for reporting fuel usage at high flow rates (Cupera and Sedlak, 2011; Marx, 2015; Marx et al., 2015). Additionally, Rohrer et al. (2018) compared the reported engine torque and engine speed from the CAN bus with measurements from a dynamometer and reported a high correlation (R2 = 99.5%) between the readings. Some examples where CAN bus data was used to analyze machine behavior include a study by Kortenbruck et al. (2017), where the authors developed a data collection and analysis methodology of machine operation states by tracking machine location using CAN bus data. Pitla et al. (2014) analyzed tractor fuel rate data and Global Positioning System (GPS) messages collected from a tractor's CAN bus to determine the field efficiencies of row crop operations. A different study collected and analyzed fuel rate, engine torque, vehicle speed, and location data from the CAN bus during various row-crop operations. The tractor field operations were categorized into three states based on distinct divisions in the collected data (Pitla et al., 2016). Therefore, ASABE standards and CAN bus data could both be practical methods for estimating power and energy requirements for actual field operations performed by battery operated or electric powered agricultural machinery.

Previous research has investigated the feasibility of electric powered agricultural equipment. Brenna et al. (2018) used theoretical equations, such as those provided in ASABE D497.7 (ASABE Standards, 2020a) and ASABE EP496.3 (ASABE Standards, 2020b), to predict the necessary power requirements for a 163-kW row-crop tractor. The authors concluded that it is economically feasible to produce, purchase, and operate an electric row-crop tractor. Unfortunately, this study did not consider the physical aspects of the volume and mass of the electric power source. Additionally, the tractor's operation was limited to only 8 hours per day, and actual field data was not used to support their analysis. Therefore, performing analysis supported by actual field data would be helpful in determining the actual energy needs and corresponding battery size currently needed to support a fully electric, high-power row-crop tractor.

This article will focus on the power and energy requirements of large-scale no-till planting operations. No-till farming is a conservation agricultural practice that improves soil health, promotes soil water retention, and reduces soil erosion (U.S. Department of Agriculture, n.d.). No-till farming has been a trend in the past two decades as farmers apply no tillage to the cropland and plant directly into the crop residue. There are as much as 36 percent of corn acres, 39 percent of soybean acres, and 45 percent of wheat acres in the US that have adopted no-till farming (Claassen, 2019; Claassen et al., 2018; Rosenberg and Wallander, 2022; Horowitz et al., 2010).

Both the ASABE D497.7 and EP496.3 (ASABE Standards, 2020a,b) standards, along with CAN bus data, will be used to calculate the total energy requirements for planting operations, with the goal of identifying a methodology to calculate power and energy demands for multiple agricultural operations. Total energy requirements for a full operating day will be calculated for up to 15 working hours per day and used to estimate the approximate size and mass of electric batteries needed to support the energy requirements for a full day of operation. The practicality of operating a hypothetical battery-powered tractor with batteries of the calculated volume and mass will also be discussed to determine the current feasibility of electric power solutions for high-power agricultural equipment.

The rest of the article is organized as follows: The methods and materials section will cover the equipment used in this study and a discussion about the ASABE and CAN-based methods for calculating power and energy requirements. The results section will present data from both methods along with battery sizing estimates. A general discussion about the methods used for power and energy calculation, along with a discussion about the feasibility of the batteries sized in this study, will be covered in the discussion section. Finally, conclusions will wrap up the article with a brief discussion of future work.

Objectives

- Use ASABE machinery management standard methodologies to calculate power requirements for the two tractor-planter configurations used in this study.
- Calculate the in-field power and energy demands of no-till corn planting operations using CAN bus data from both tractor-planter configurations in this study.
- Estimate the kWh capacity and physical size (mass and volume) of the battery power source required to power a hypothetical fully electric row-crop tractor for planting.

Materials and Methods

Equipment Used

Planting is one of the most important agriculture operations for row-crop farmers since it is a major step in determining the yield potential for a given crop. For this study, two tractors and two corn planters (fig. 1) were chosen for analysis and labeled Case A and Case B throughout the study. A summary of the tractor and planter specs for each scenario can be found in table 1. Both methods for power and energy calculation were performed on each of these tractor-planter configurations for no-till corn planting operations throughout the full planting seasons (in two different years, with 23 fields in total). In no-till field conditions, the seed is planted into firmer soil in the presence of crop residue, making no-till planting more power-demanding than conventional planting. This study allows us to look at the planting energy requirement with the worst-case scenario.

In-field CAN bus data was collected for the second analysis method in this study. The primary CAN bus data during planting was collected using Farmobile PUCs (Passive Uplink Connection Generation 4, Farmobile, LLC, Overton, KS, USA), as shown in figure 2. The PUC devices were connected to the tractor diagnostics port located inside the tractor cab, which wirelessly transmitted data to Farmobile DataEngine cloud servers at 1 Hz frequency (DataEngine, Farmobile, LLC, Overton, KS, USA) using a cellular connection. The data was summarized as either a shape file or comma separated value (CSV) file and was available for download. Farmobile PUC allowed ease of data collection over cloud and had the ability to extract data without the need to physically access the device. The data process flow can be seen in figure 3, where more details on data processing will be given later in this section.

Farmobile PUCs only recorded a list of the selected messages from the CAN bus. An additional CAN data logger, Kvaser Memorator (Memorator Pro 2xHS, Kvaser AB, Mölndal, Sweden), was used to collect the missing messages, namely, SAE J1939 Engine Configuration 1, as shown in figure 4. This message was particularly important to compute the actual gross engine power as it contained the reference torque information. The reference torque data of the engine is a constant number and is not dependent on the load demands of field operations. This data was collected in static conditions during the non-planting period and was stored on an SD card of the data logger for post processing.

Figure 1. Tractors and Planters used. (Top: Case A, John Deere 7250R, with 1775NT 16-row central fill planter, Bottom: Case B, CLAAS Xerion 5000, with DB120 48-row central fill planter).

Table 1. Equipment specifications of Case A and Case B in this study are listed in this table.

Equipment Specification	Case A	Case B
Tractor	John Deere 7250R	CLAAS Xerion 5000
Rated Power (kW (hp))	186 (250)	386 (517)
Drive Type	Mechanical Front Wheel Drive (MFWD) with duals	4-Wheel Drive (4WD) with duals
Number of Front Wheels	2	4
Number of Rear Wheels	4	4
Front Axle Load[a] (kg)	3572	10789
Rear Axle Load[a] (kg)	7121	8834
Front Tire Specifications	420/90R30 Firestone Radial All Traction FWD Tractor Tire (16.9R30)	710/70R42 Firestone Radial All Traction DT Tractor Tire
Rear Tire Specifications	480/80R46 Firestone Radial Deep Tread Tractor Tire (18.4R46)	710/70R42 Firestone Radial All Traction DT Tractor Tire
Planter	John Deere 1775NT	John Deere DB120
Number of Rows	16	48
Row Spacing (mm (inch))	762 (30)	762 (30)
Recommended Minimum Tractor Power (kW (hp))	90 (120)	272 (365)

[a] Values taken from Nebraska Tractor Test Lab, unballasted static load with operator (Nebraska Tractor Test Lab, 2014, 2017)

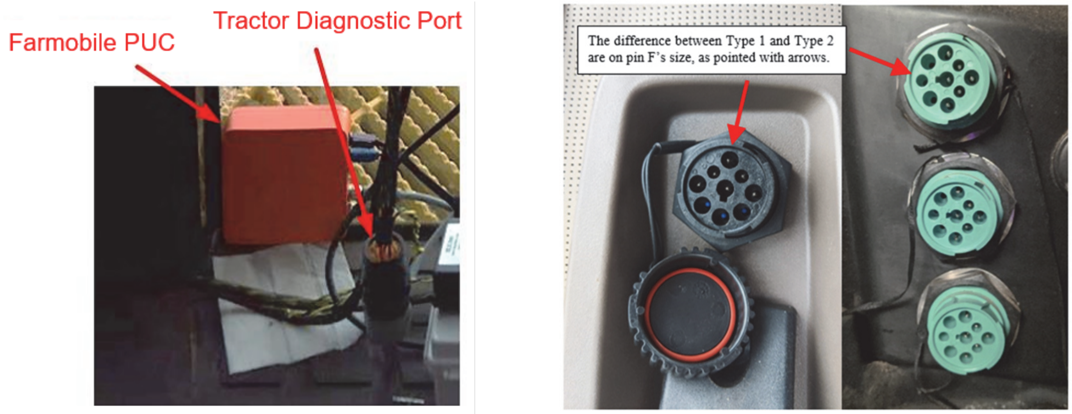

Figure 2. (Left) Farmobile PUCs are located inside the cab and connected to tractor diagnostic port; (Right) The tractor diagnostic port located inside the cab. Depending on the tractors, there can be either type 1 or type 2 connectors, which are for two different baud rates, namely 250 kbit/s and 500 kbit/s, respectively, on the tractor bus.

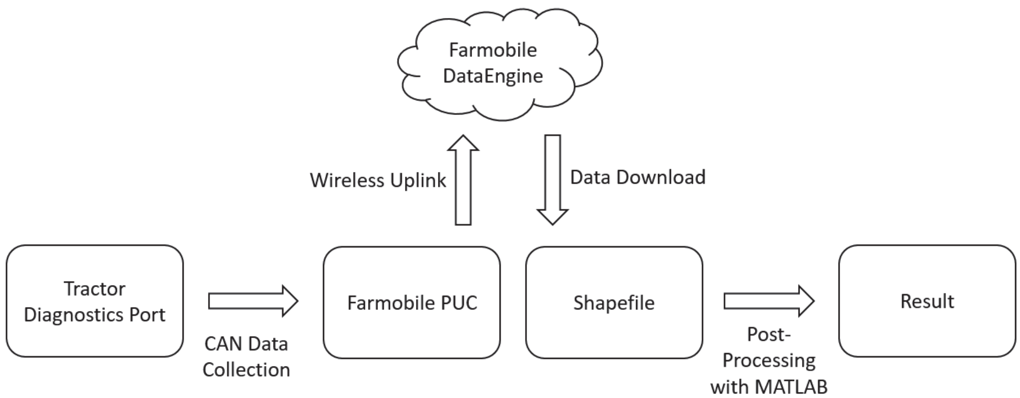

Figure 3. Data process flow from CAN data collection from the tractor via Farmobile, and the post-processing and analysis with MATLAB.

Figure 4. Kvaser Memorator Pro 2x HS installed on the tractor diagnostic connector to log the CAN data stream.

Theoretical Energy and Power Calculations Using ASABE/ASAE Standards

Before analyzing the collected CAN bus data, theoretical power demands for the planting operations in this study were first calculated using ASAE D497.7 and ASAE EP496.3 standards (ASABE Standards, 2020a,b). The goal of the theoretical calculations was to determine the equivalent Power Take-Off (PTO) power and gross engine power required from the tractor to support the planting operation. ASAE standard EP496.3 provides the equations needed to calculate equivalent PTO power for an operation in clauses 4.2 and 4.3 (eq. 1). The equation is a sum of the drawbar, PTO, hydraulic, and electrical power demands of an operation.

$$P_T = \frac{P_{db}}{E_m E_t} + P_{pto} + P_{hyd} + P_{el} \quad (1)$$

where

P_T = total implement power requirement or equivalent tractor PTO power, kW

E_t = tractive efficiency of the tractor (expressed as a decimal) (see ASAE D497.7, clause 3)

P_{db} = drawbar power required for the implement, kW

P_{hyd} = hydraulic power required by the implement, kW

P_{pto} = power take-off power required by the implement, kW

P_{el} = electric power required by the implement, kW

E_m = mechanical efficiency of the transmission and power train. This coefficient is typically 0.96 for tractors with gear transmissions.

According to ASAE D497.7 clause 3, tractive efficiency (E_t) can either be estimated from the table in clause 3.1 (as shown in table 2) or calculated using equations 2-5 found in clause 3.2. Since this study is looking to perform an accurate calculation of the total power required for a planting operation, equations 2-5 were used instead of the estimated tractive conditions in table 2.

Table 2. Tractive Condition factors, referenced as E_t in ASAE EP496.3 clause 4.2 or TE in ASAE D497.7 clause 3.1.

Tractor Type	Tractive Condition			
	Concrete	Firm	Tilled	Soft
2WD	0.87	0.72	0.67	0.55
MFWD	0.87	0.76	0.72	0.64
4WD	0.88	0.77	0.75	0.70
Track	0.88	0.76	0.74	0.72

$$B_n = \left(\frac{CI\ b\ d}{W}\right)\left(\frac{1+5\frac{\delta}{h}}{1+3\frac{b}{d}}\right) \tag{2}$$

where
B_n = a dimensionless ratio
W = dynamic wheel load normal to the soil surface (kN)
CI = cone index for the soil (kPa) = 1200 for firm soil
b = unloaded tire section width (m)
d = unloaded overall tire diameter (m)
h = tire section height (m)
δ = tire deflection (m)
s = slip (decimal); see ASAE S296.

$$NT = \sum nt_n = \sum W_n \left(0.88\left(1-e^{-0.1B_n}\right)\left(1-e^{-7.5s}\right) - \frac{1}{B_n} - \frac{0.5s}{\sqrt{B_n}}\right) \tag{3}$$

where
NT = net traction as defined in ASAE S296 (kN)
nt_n = net traction of the n'th wheel (kN)
W_n = dynamic wheel load normal to the soil surface (kN)
B_n = a dimensionless ratio; see equation 3
s = slip (decimal).

$$GT = \sum gt_n = \sum W_n \left(0.88\left(1-e^{-0.1B_n}\right)\left(1-e^{-7.5s}\right)+0.04\right) \tag{4}$$

where
GT = gross traction as defined in ASAE S296 (kN)
gt_n = gross traction of the n'th wheel (kN)
W_n = dynamic wheel load normal to the soil surface (kN)
B_n = a dimensionless ratio, see equation 3
s = slip (decimal).

$$E_t = (1-\ s)\frac{NT}{GT} \tag{5}$$

where
E_t = tractive efficiency of the tractor (expressed as a decimal) (see ASAE D497.7, clause 3)
GT = gross traction as defined in ASAE S296 (kN)
NT = net traction as defined in ASAE S296 (kN)
s = slip (decimal).

Table 3 lists tire parameter values, dynamic wheel load (W), and slip values used to calculate tractive efficiency for each tractor using equations 2-5. These values were gathered from tractor testing (Nebraska Tractor Test Lab, 2014, 2017) and tire manufacturing specifications for the respective tractors used in this study (Firestone, n.d.-a,b,c). Since the tire parameters for the front and rear tires on each tractor can vary, motion resistance for the front and rear tires was calculated separately and summed together to calculate a total tractive efficiency factor for each tractor. Wheel slip for both tractors, as defined in ASAE S296, will be assumed to be 0.12, as suggested by Shelton and Rider (2014).

Drawbar power (P_{db}) was calculated using equations 6-7. According to ASAE EP496.3 clause 4, the motion resistance of the implement wheels can be factored into the total drawbar power equation if the implement is assumed to be operating on soft or loose soils. Since this study assumes firm soils, the motion resistance of the implement tires will be considered negligible. Therefore, equation 6 is only based on the draft force of the planter itself, which varies based on implement type, implement width, and soil conditions.

$$P_{db} = \left(\frac{D}{3600}\right)v \tag{6}$$

where
P_{db} = total drawbar power required (kW)
D = draft force to pull the planter (N)
v = tractor velocity (km h^{-1}).

$$D = \left[F_i\left(A+Bv+Cv^2\right)KT\right]*\left(1\pm 25\%\right) \tag{7}$$

where
D = draft force to pull the planter (N)
K = number of tools (integer)
F_i = dimensionless soil texture adjustment parameter = 1
i = 1 for fine, 2 for medium, and 3 for coarse textured soils
A = machine parameter = 1,820 N
B, C = machine parameter = 0
v = field speed (km h^{-1}) = according to actual operation speed
T = tillage depth (cm) = 1 (dimensionless) for minor tillage tools and seeding implements.

There is a ±25% range of the estimated implement draft force to be included per ASAE D497.7 clause 4.1.2 and table 1 to account for "differences in machine design, machine adjustment, machine age, and site-specific conditions including soil moisture and residue cover."

Equation 1 includes terms for power take-off (P_{pto}), hydraulic (P_{hyd}), and electric powers (P_{el}); however, the ASABE standard does not provide any information or calculation for estimating those three terms. Therefore, these terms were excluded from the overall power calculation (eq. 1). After calculating the total implement power requirement (P_T), an additional 20 percent could be added to P_T to account for reserve power when sizing tractors for the operation (ASAE EP496.3 clause 4.3). Since this study will compare the calculated power demands to the recorded power demands from the CAN bus data, the 20 percent power addition will be left out to allow for an even comparison with the gross power demands from the CAN data. This results in the total power needed to support the agricultural operation of interest. A summary of the process taken to calculate power requirements for the planting operations in this study can be found in figure 5. The efficiency value to convert between equivalent PTO power (P_T) and gross engine power

Table 3. Motion resistance calculation for each tractor.

Tractor and Field Parameters	Case A: John Deere 7250R		Case B: CLAAS Xerion 5000	
	Front	Rear	Front	Rear
Tire Model	420/90R30 Firestone Radial All Traction FWD Tractor Tire (16.9R30)	480/80R46 Firestone Radial Deep Tread Tractor Tire (18.4R46)	710/70R42 Firestone Radial All Traction DT Tractor Tire	710/70R42 Firestone Radial All Traction DT Tractor Tire
Tires	2	4	4	4
W_n[a] (kN)	17.5	17.5	26.5	21.7
CI[b] (kPa)	1200		1200	
B[c] (m)	0.44	0.49	0.72	0.72
D[c] (m)	1.49	1.96	2.05	2.05
H[c] (m)	0.36	0.40	0.49	0.49
S[d] (decimal)	0.12		0.12	
δ[c] (m)	0.07	0.08	0.11	0.11
B_n (-)	45.7	76.0	69.5	83.9
nt_n (kN)	8.52	8.77	13.23	10.92
gt_n (kN)	9.76	9.81	14.86	12.18
NT (kN)	52.1		96.6	
GT (kN)	58.8		108	
E_t	0.78		0.79	

[a] Obtained from NTTL Reports (Nebraska Tractor Test Lab, 2014, 2017)
[b] ASAE D497.7 (3.2.1.1)
[c] Obtained or derived from tire specification (Firestone, n.d.-a,b,c)
[d] Defined in ASAE S296 and recommended from Shelton and Rider (2014)

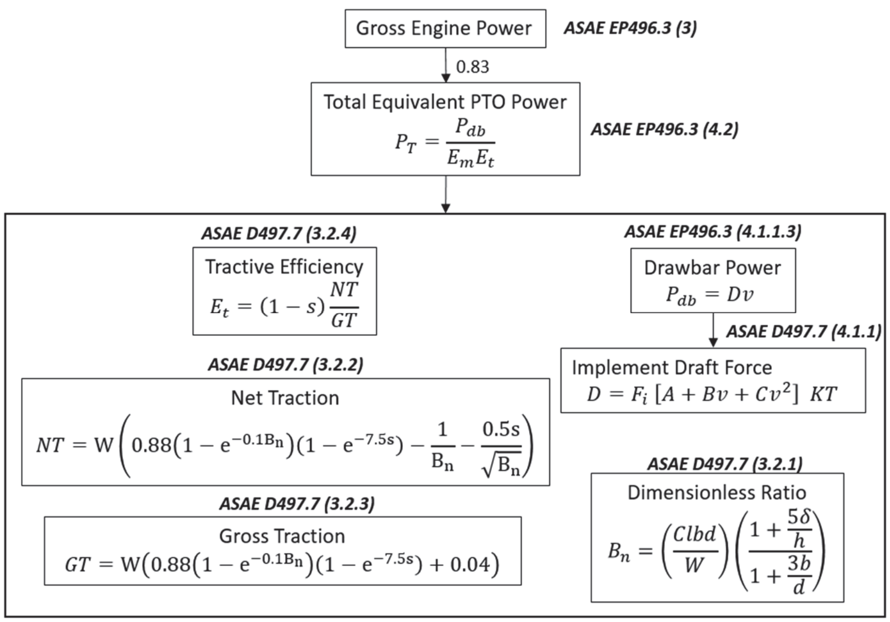

Figure 5. Power and energy calculation process for planting using the ASAE EP496.3 and ASAE D497.7 machinery standards. This is the compilation of equations 1 to 7.

can be seen at the top of the figure. The efficiency value allows for the comparison of gross engine power requirements and demands as determined from the ASABE and CAN methods, respectively.

Energy and Power Calculations Using CAN Bus Data

The parsing of tractor CAN bus data is a meticulous task; therefore, a sequence of steps was followed for calculating average power demands during planting operations and total energy consumption for each operating day. The first step in this study was to gather CAN bus data files from Farmobile's DataEngine cloud server (DataEngine, Farmobile, LLC, Overton, KS, USA). Farmobile organizes the collected CAN bus data by day. Because the data was recorded by day, it was important to identify the dead space where the tractor was not turned on, which was indicated by a time interval greater than 10 seconds between two successive data points. Then, the data per day was sliced into multiple operating segments per day. This step was important as finding the actual operating data had an impact on the energy demand calculation. Table 4 lists the CAN messages of interest for this study and a set of parameters used for post-processing and analysis. MATLAB was used for the data processing in this study since it provided many tools for filtering and parsing large amounts of data.

Unfortunately, CAN data does not report the engine power demands directly. To calculate the engine power demands for the planting operations in the recorded CAN data, three data series were required: engine percent torque, engine speed, and reference torque. Engine percent torque and engine speed are found from the Farmobile dataset. Engine

Table 4. The parameters used in this study: The operating data was collected using Farmobile during planting, and Kvaser Memorator was used to collect engine reference torque data.

Parameters	Unit	Description	PGN	SPN	Source
Latitude	Degree	Latitude defined by PUC GPS	-	-	Farmobile DataEngine
Longitude	Degree	Longitude defined by PUC GPS	-	-	Farmobile DataEngine
Time Stamp	Date-Time	Timestamp when data was collected in the field	-	-	Farmobile DataEngine
Ground Speed	mph	Ground speed defined by PUC GPS	-	-	Farmobile DataEngine
Vehicle Speed	mph	Vehicle speed calculated from wheel or tail shaft speed	65265	84	Farmobile DataEngine
Hitch Height	%	Rear Hitch Position in range of 0-100%	65093	1873	Farmobile DataEngine
Engine Speed	RPM	Engine Speed in RPM defined by engine ECU	61444	190	Farmobile DataEngine
Engine Torque	%	Engine torque in percentage of the engine reference torque, defined by engine ECU	61444	513	Farmobile DataEngine
Average Population	Seeds per acre	Average seed population given by seed sensor	-	-	Farmobile DataEngine
Engine Reference Torque	Nm	The reference torque in Nm for which the engine percent torque is referring.	65251	544	Kvaser Memorator

percent torque is reported as a percentage of the reference torque. However, reference torque, found in SAE J1939 standard parameters, did not exist in the Farmobile dataset and therefore was collected using a separate data logger (Memorator Pro 2xHS v2, Kvaser AB, Mölndal, Sweden). Reference torque on the CAN bus is an arbitrary, fixed reference value; therefore, it was only necessary to find the value once when performing power calculations. Reference torque was identified as 1080 Nm for the John Deere 7250R (Case A) and 2666 Nm for the CLAAS Xerion 5000 (Case B).

$$P = \frac{T_p}{100} T_{ref} \omega_{rpm} \frac{2\pi}{60} \tag{8}$$

where

P = power produced by the engine (W)

T_p = reported percent torque (%)

T_{ref} = reference torque (Nm) reported by SAE J1939 standard

ω_{rpm} = reported engine speed (RPM).

Equation 8 was used to calculate engine power demands. The resulting power demands represent gross engine power since percent engine torque was measured before parasitic losses (SAE International, 2022; Rohrer et al., 2018). The last step in analyzing the CAN data in this study was to integrate the engine power demands over time to get an accurate measurement of total energy demands for a full operating day. Numerical integration of the power data was performed using MATLAB's "trapz" function. Figure 6 demonstrates the integration of power data to calculate cumulative energy usage over the selected time window.

Battery Sizing Based on Energy Requirements

To estimate the required battery pack size and mass to support the energy demands of the planting operation, Tesla 18650 battery modules were explored for energy capacity, mass, and volume. One Tesla battery module contains 444 lithium-ion cells, a cooling system, connectors, and an enclosure. The 18650 battery pack specifications are summarized in table 5.

Battery module volume can be estimated using the volumetric energy density of a battery.

$$Volume\left(m^3\right) = \frac{Energy\ Required\left(kWh\right)}{Volumetric\ Energy\ Density\left(kWh\, m^{-3}\right)} \tag{9}$$

Similarly, the mass of the battery module needed can be estimated using the specific energy density.

$$mass\left(kg\right) = \frac{Energy\ Required\left(kWh\right)}{Gravimetric\ Energy\ Density\left(kWh\, kg^{-1}\right)} \tag{10}$$

These two equations, along with the Tesla 18650 battery module properties, will be used to estimate the total volume and mass of a battery pack needed to support all days of operation of a fully electric tractor.

Results and Discussion

Theoretical Energy and Power Requirements for Planting

Total gross power requirements were calculated using the ASABE standards as previously outlined. Table 6 displays power demands for each case, dependent on the speed of operation. Three ranges were given for the power requirements since equation 5 contains a ±25% factor for draft force.

When comparing both the ASABE and CAN data methods for power requirements, it is useful to break down the total power requirements on a per-row basis. Since Case A operates with a 16-row planter and Case B with a 48-row planter, total power requirements can be divided by the respective row number to get average power per row. Table 7 presents the per-row power requirements for each case across multiple operating planting speeds.

CAN Bus Reported Data and Operation Modes Separation

Twelve and eleven days of CAN bus data were collected for Cases A and B, respectively. The data were categorized into four operation modes: planting, headland, transport, and stoppage. Figure 7 shows partial data of 150 minutes from engine power, engine rpm, tractor ground speed, and seeding rate of an operating day of Case A, which contains the four operation modes.

Planting mode can be easily identified by monitoring the seed population. When the seeding rate was greater than zero, a planting operation was performed. Planting mode is labeled in green in figure 7, where the engine power is consistently high at around 120 kW (161 hp) with the seeding rate at about 74,132 seeds per ha (30,000 seeds per acre), and the engine speed is around 1600-1700 rpm. Blue labels are

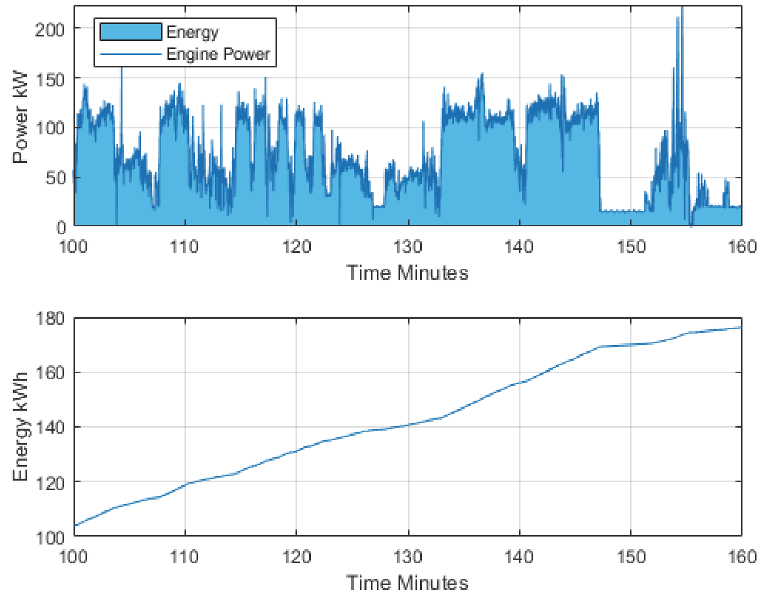

Figure 6. (Top) Engine Power (dark blue) is plotted over time with area under the curve (light blue) representing the energy demand over 60 minutes of partial data; (bottom) the cumulative energy of the same 60 minutes of the top chart, the integration of the power resulting in the total energy need.

Table 5. Battery Module Information.

Specifications	Tesla 18650 Battery Module[a]
Height (m)	0.08
Width (m)	0.30
Depth (m)	0.67
Usable energy (kWh)	5.3
Mass (kg)	25.0
Volumetric Energy Density (kWh m^{-3})	335
Gravimetric Energy Density (kW kg^{-1})	0.21

[a] (Bhowmick, 2021)

Table 6. Total drawbar power requirements using ASABE method (kW).

	Drawbar power range (D), kW					
	Case A			Case B		
Planting Speed (v), km h^{-1}	Lower Bound (-25%)	Nominal	Upper Bound (25%)	Lower Bound (-25%)	Nominal	Upper Bound (25%)
1	9.8	13.0	16.3	29.1	38.8	48.4
2	19.5	26.0	32.5	58.1	77.5	96.9
3	29.3	39.0	48.8	87.2	116.3	145.3
4	39.0	52.1	65.1	116.3	155.0	193.8
5	48.8	65.1	81.3	145.3	193.8	242.2
6	58.6	78.1	97.6	174.4	232.5	290.7
7	68.3	91.1	113.9	203.5	271.3	339.1
8	78.1	104.1	130.1	232.5	310.0	387.5
9	87.8	117.1	146.4	261.6	348.8	436.0
10	97.6	130.1	162.7	290.7	387.5	484.4
11	107.4	143.2	178.9	319.7	426.3	532.9
12	117.1	156.2	195.2	348.8	465.0	581.3

headland turns (which can be seen in between the green planting data), and orange labels are transport (which can be seen as a short spike of engine power, engine speed, and ground speed). Lastly, purple labels are stoppage, which corresponds to the situation where the tractor is stopped and not moving. The same data from figure 7 is shown as a map in the fields in figure 8, where the planting operation occurred, using the same color codes for each operation mode.

Table 7. Total gross power requirements per row ASABE method (kW row^{-1}).

	Gross engine power range (P_T), kW row^{-1}					
	Case A			Case B		
Planting Speed (v), km h^{-1}	Lower Bound (-25%)	Nominal	Upper Bound (25%)	Lower Bound (-25%)	Nominal	Upper Bound (25%)
1	0.61	0.81	1.02	0.61	0.81	1.01
2	1.22	1.63	2.03	1.21	1.61	2.02
3	1.83	2.44	3.05	1.82	2.42	3.03
4	2.44	3.25	4.07	2.42	3.23	4.04
5	3.05	4.07	5.08	3.03	4.04	5.05
6	3.66	4.88	6.10	3.63	4.84	6.06
7	4.27	5.69	7.12	4.24	5.65	7.06
8	4.88	6.51	8.13	4.84	6.46	8.07
9	5.49	7.32	9.15	5.45	7.27	9.08
10	6.10	8.13	10.17	6.06	8.07	10.09
11	6.71	8.95	11.18	6.66	8.88	11.10
12	7.32	9.76	12.20	7.27	9.69	12.11

Energy Requirements and Operating Hours

After filtering out downtime hours for each day, total hours of operation were separated into planting, headland turn, transport, and stoppage. Table 8 presents the total operating hours for each day of the actual field data collected in this study. It is interesting to note that the average daily hours of operation were 6.9 and 8.2 hours for cases A and B respectively, while the respective maximum operating hours were 13.7 and 14.8 hours for cases A and B. Previous research studies, such as Brenna et al. (2018), have assumed an eight-hour workday when making total energy calculations for agricultural operations. Although an 8-hour workday may be a valid average value across many operations, it does not account for the increased working hours during critical time periods such as planting and harvest. The dataset that this study provided demonstrates that working days as long as 14-15 hours could be possible during critical periods of the year. Electric power solutions would need to have the capability to support these long working hours;

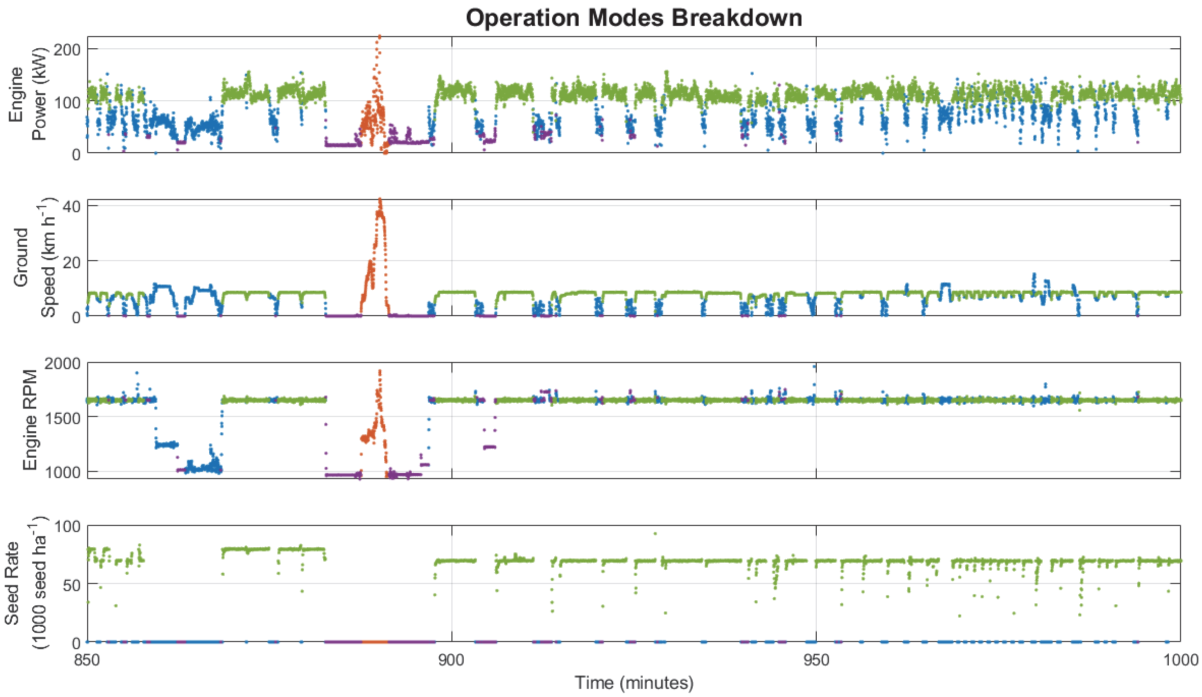

Figure 7. The partial data of the four important parameters over 150 minutes of a planting day in Case A are shown. The parameters from top to bottom are engine power (kW), ground speed (km h^{-1}), engine speed (RPM), and seeding rate (1000 seeds ha^{-1}). The data are separated into four modes as indicated by colors: green=planting, blue=headland turn, orange=transport, and purple=stoppage.

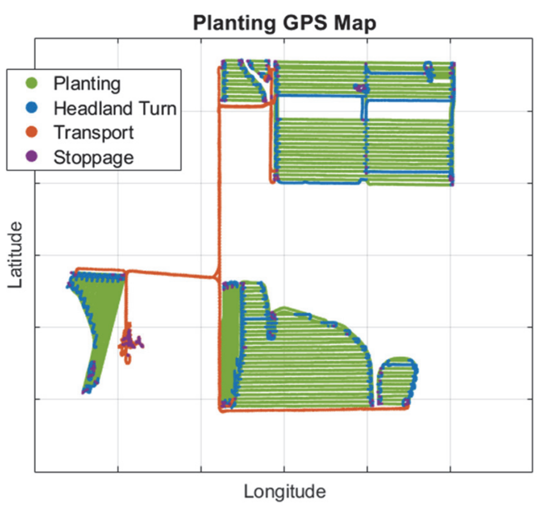

Figure 8. The GPS map of a planting day with color-coded operation modes of the tractor: green=planting, blue=headland turn, orange=transport, and purple=stoppage.

Table 8. Hours Operated and Energy Used Calculated from CAN Data and the planted area per day.

	Case A: JD7250R+1775NT			Case B: CLAAS Xerion 5000+DB120		
Planting Day	Case A Usage (h)	Energy (kWh)	Planted Area (ha)	Case B Usage (h)	Energy (kWh)	Planted Area (ha)
1	1.00	24	0.0	2.16	120	0.0
2	2.22	110	3.9	8.61	1170	66.9
3	13.74	1117	67.9	7.90	623	38.8
4	9.46	813	50.9	11.33	1787	115.1
5	9.85	822	53.3	4.94	528	25.7
6	6.59	529	35.7	6.46	678	29.3
7	6.88	458	26.0	14.62	2483	158.1
8	5.58	414	25.4	9.16	1636	120.7
9	1.56	57	0.5	6.20	1034	45.3
10	10.06	836	57.2	6.60	1121	47.3
11	4.64	315	18.3	2.74	389	10.1
12	11.20	955	63.0	--	--	-

therefore, sizing batteries that can support these energy demands is important.

After integrating daily power demands for each day, the total energy values were tabulated to show energy use over each day. Table 8 also lists the energy usage and planted area for each day. Note that both cases A and B conducted trial planting on day 1, where the seeds were not planted on an actual plot. On day 9 for Case A, only 0.5 ha was planted due to the weather conditions on that day.

Figure 9 presents a time breakdown for each day of recorded CAN bus data into the four operation modes. The longest working hours recorded were 13.7 hours on day three for Case A and 14.8 hours on day seven for Case B. On average, Case A tractor spent 42%, 11%, 11%, and 36%; Case B tractor spent 24%, 14%, 10%, and 53% of their daily operating time on planting, headland turn, transport, and stoppage, respectively. Note that Case B contained a high amount of stoppage in between planting modes due to adjustments needed to the planter.

The daily operation energy demands for the four modes are shown in figure 10. Case B consists of a larger tractor and a wider planter, and thereby spent more energy than Case A. The highest energy usages were 1117 kWh on day three for Case A and 2658 kWh on day seven for Case B. On average, Case A tractor spent 62%, 10%, 11%, and 17%; Case B tractor spent 46%, 19%, 10%, and 25% of their daily energy for planting, headland turns, transport, and stoppage, respectively.

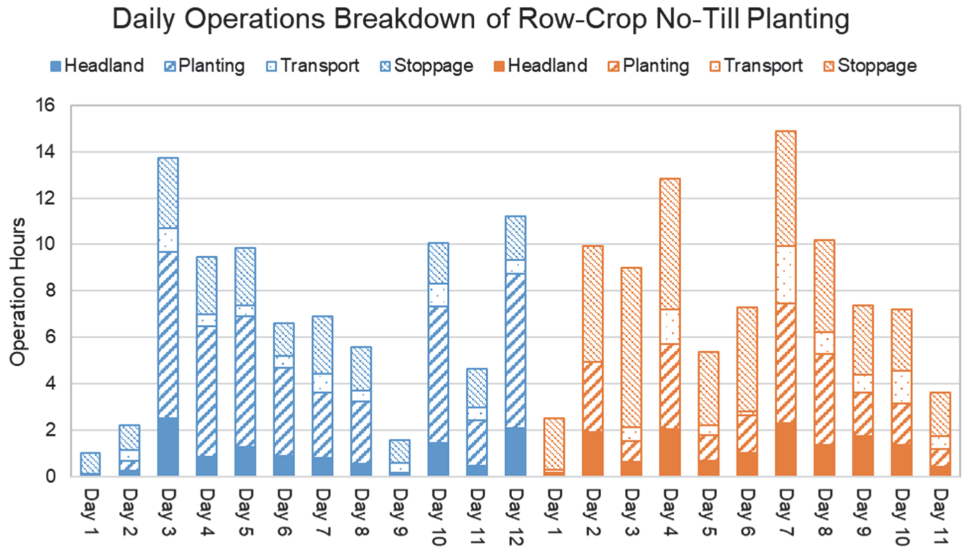

Figure 9. Breakdown of the total daily operation time of Case A (blue, left) and Case B (orange, right) into planting, headland turn, transport, and stoppage.

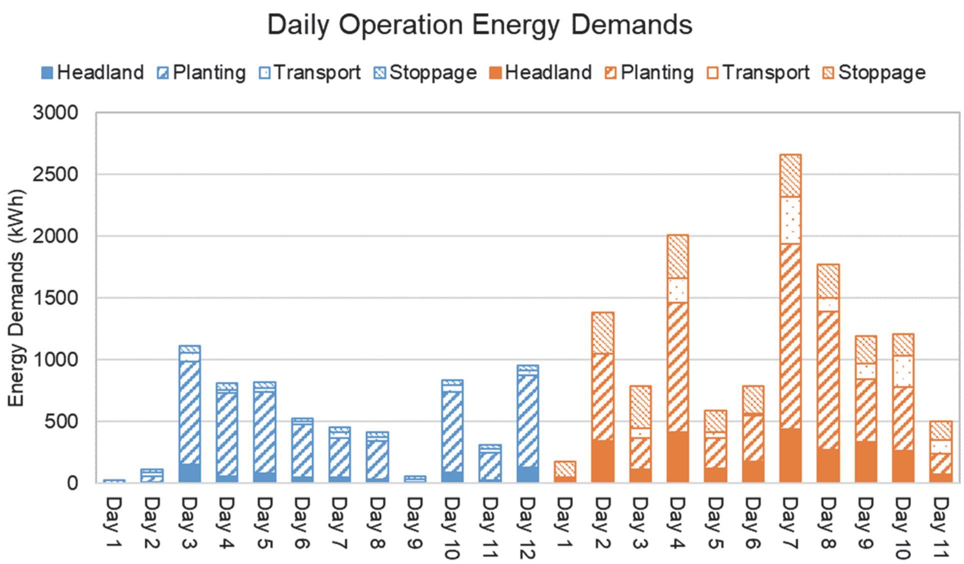

Figure 10. The daily energy demands of Case A (blue, left) and Case B (orange, right) for the four operation modes: planting, headland turn, transport, and stoppage.

CAN Reported Power Demands for Planting Mode

Table 9 presents the daily average power demands per row and operating speed during planting mode calculated from CAN bus data. Case A's daily average planting speed is between 7.9 km h^{-1} (4.9 mph) and 8.56 km h^{-1} (5.3 mph), whereas Case B has a wider range of daily average planting speed between 3.97 km h^{-1} (2.5 mph) and 8.88 km h^{-1} (5.5 mph). The planting power was divided by the number of row units for a valid comparison between 16-row and 48-row planters at similar speeds. Note that the planting speed has a major impact on the planting power per row. These values can be compared to the ASABE-calculated power requirements for different planting operation speeds.

ASABE and CAN Power Demands Comparison

Power and energy demands were comparable between the ASABE and CAN calculation methods. Figure 11 presents

Table 9. Daily average ground speed during planting and daily average planting power per row calculated from CAN bus data. Note that the planting power per row is dependent on planting speed.

	Case A: JD7250R+1775NT		Case B: CLAAS Xerion 5000+DB120	
Planting Day	Daily Average Planting Speed (km h^{-1})	Power per Row (kW row^{-1})	Daily Average Planting Speed (km h^{-1})	Power per Row (kW row^{-1})
1	7.90	6.42	3.97	4.59
2	8.27	6.51	4.12	4.69
3	8.56	7.23	7.44	5.98
4	8.56	7.81	7.37	6.06
5	8.34	7.27	4.12	4.59
6	8.27	6.98	4.83	4.80
7	8.27	6.97	8.88	6.16
8	8.27	7.26	8.20	5.96
9	8.18	6.96	7.41	5.66
10	8.56	6.80	7.66	5.84
11	8.38	6.88	5.01	4.49
12	8.56	6.99	-	-

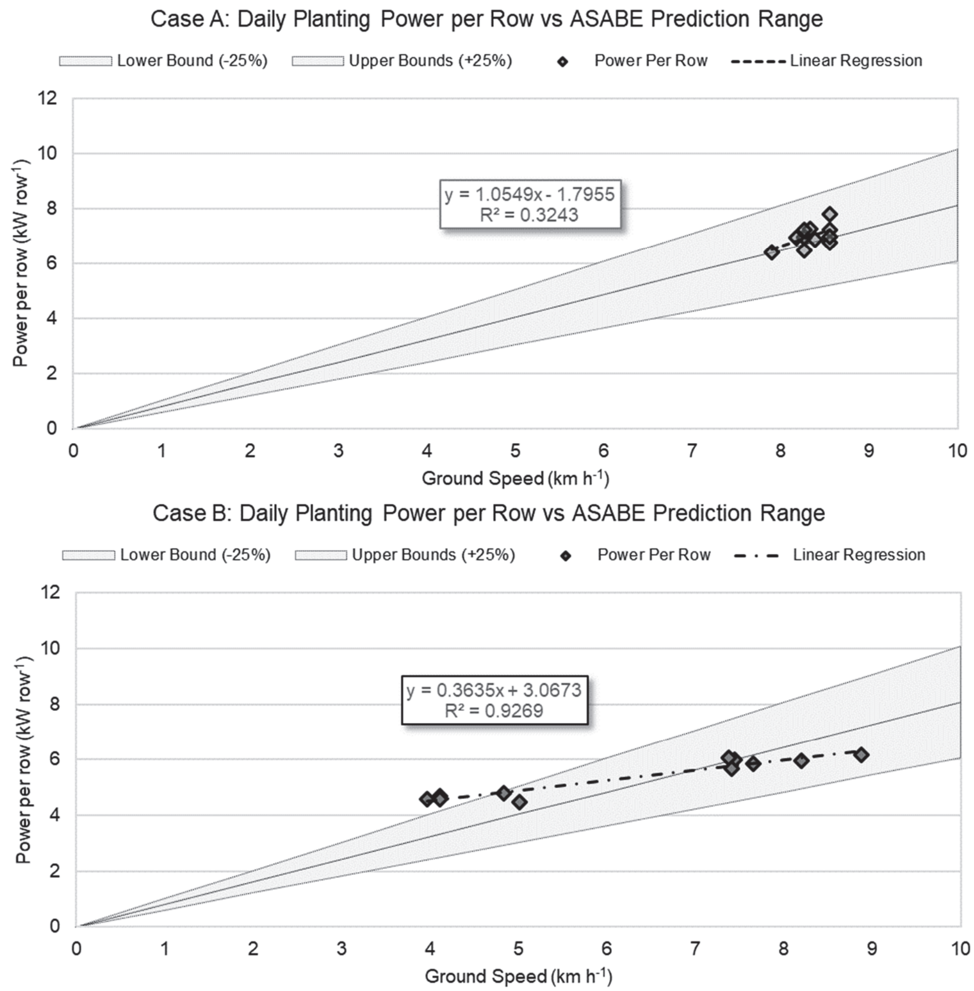

Figure 11. Daily power demands per row versus planting speed for Case A (top) and Case B (bottom). The shaded zones are the ±25% range from the ASABE estimation. Due to the narrow range of speed, the linear regression of Case A has a low R-squared score, but well within the ASABE estimation. On the other hand, Case B has a good linear regression fitting, but at low planting speed, the planting power per row exceeded the ASABE estimation.

two graphs for each scenario in this study. The shaded area in the top graph shows ranges of power that Case A could require based on ASABE calculations. The ASABE estimation given for planting operations only considers drawbar power, which itself linearly correlates with ground speed, without y-intercept, and has an estimated power usage of zero at rest. Modern row-crop planters often require 2-5 hydraulic ports for the seed delivery system and downforce adjustment. However, the ASABE calculation does not provide any information on the power demands from the hydraulic and electrical systems. Additional hydraulic and electric power demands are to be expected on top of the estimated ASABE power requirements if hydraulic and electric power demands from the planter are included.

On the same chart (fig. 11), daily data points from the collected CAN data were plotted. Each data point represents the average planting speed and planting power per row for each day of the collected CAN data. A linear trendline was fitted to the CAN data points to demonstrate the relative trend for Case A. Since the planting operations in Case A were performed across a narrow range of planting speeds (±0.5 kmh^{-1}) and there are variations among the averaged power across the planting day, the linear trend-line showed an R-squared score of only 0.3243.

Case B is represented on the bottom graph in figure 11. The ASABE power per row estimations are similar in Case B. Again, the daily average power per row and planting speed for Case B were plotted on the second graph. Because the planting operations performed in Case B included a much wider variation in average planting speeds, the trend-line has a better fit to the actual operation conditions, with an R^2 score of 0.9269. It is interesting to note that the trend-line in the second graph has a y-intercept value greater than zero. This implies the planting operation would need non-zero power per row even when the planter is not moving. There are multiple factors that contribute to tractor power usage. As planting drawbar power typically increases linearly with the ground speed, the hydraulic and electric power for the planter might or might not be correlated to the ground speed linearly. In addition, there are parasitic loads and auxiliary power consumptions from the tractor, such as air-conditioning, engine cooling fan, etc., that are not linear to the ground speed.

Despite the missing terms of hydraulic and electric power from the ASABE estimation, most of the data points for the

CAN data in each study fall within the predicted ASABE power requirement range with minor deviations from the ASABE prediction range. Case B power per row at a lower planting speed exceeded the ASABE range of predictions. The possible explanations for the discrepancies at low planting speed in Case B could be that planting at low speed is inefficient, the missing hydraulic and electrical terms might contribute to the power difference, and the tractor power usage became dominant at low speed. Note that this study only utilized two tractor/planter setups, which would be insufficient to prove or disprove the effectiveness of ASAE EP496.3 and ASAE D497.7 machinery management standards. However, from the standpoint of sizing the tractor for row-crop planting, the tractor's power requirement would have been selected based on the highest planting speed. Thus, the ASAE predictions are considered valid and could be used for estimating the power requirements of current-day planting operations.

Energy Requirement Per Planting Area

An alternative method for estimating the required energy for planting operations is to look at the planted area. A major incentive for using a larger, more powerful row-crop tractor and a wider planter is to be able to plant more area in a shorter amount of time. The relationship between energy usage and the planted area and the energy efficiency of different planter widths was investigated. Thus, this section explores the correlation between the daily energy requirement and the planted area.

Figure 12 shows the planting energy usage against the daily planted area in hectare of Case A (top) and Case B (bottom). The energy used for (1) planting only and (2) planting and headland turn were considered. The energy for moving the tractor between plots, the tractor's stoppage, and idle energy losses were not included. In all cases, the energy usage showed a high correlation, and linear trendlines are a good fit with the planted area. The four linear trendline equations can be used to infer the energy scaling with the planted area. Table 10 listed the energy scalers from the best-fit-curves in figure 12, which showed that the wider planter had a lower energy usage per planted area, despite the wider planter also using more energy during headland turn. These numbers can be inversed to determine the area of land that can be planted given the battery capacity, which is 7.19 ha (17.8 acres) per 100 kWh for Case A and 7.81 ha (19.3 acres) per 100 kWh for Case B when considering planting plus headland turn. Note that the amount of time and energy spent during headland turns for the planter depends on the field size and shape; wider planters generally suffer from lower field efficiency when planting in an irregularly shaped field and waste more time and power maneuvering the planter within the field and during turns in the headland. The energy expenditure of a wider planter during headland turns is generally higher than that of a narrower planter. However, by looking at the amount of energy expenditure per planted hectare, our Case B gains a small but marginal energy efficiency. Note that this data is shown in terms of daily planted area and daily planting energy expenditure; the effect of individual fields was not considered. The numbers here allow an estimation of battery size depending on the desired planting area.

Battery Sizing

The battery sizes needed for this study were estimated using the days with the highest energy demand. For Case A, this happened on day three, where 68 hectare (168 acres) were planted, whereas for Case B, it occurred on day seven, where 158 hectare (391 acres) were planted. Based on the energy densities for the Tesla 18650 battery module in table 5, assuming without recharging, the required battery mass and volume are summarized in table 11. Figure 13 also depicts the size of battery needed relative to a 1.8 meter (six-foot) tall person. The battery sizing and mass are based on the specifications for the Tesla 18650 battery modules and do not include additional sizes of battery management systems, inverters, or other electrification accessories; therefore, the needed battery size would be larger than the sizes listed.

Another consideration regarding battery sizing is the cooling and thermal management capabilities, as the Tesla battery pack has its cells arranged in a planar formation and contains a built-in active cooling system. It is unknown how the scaling of the thermal condition would be if the battery were to stack differently. In this article, we assume the scaling to be linear with the volume.

Electric Charging Capabilities

There are multiple EV charging standards available on the market. Earlier charging standards consist of Level 1 and Level 2 charging, which transfer the electricity to EVs over AC power and offer up to 1 kW and 7 kW charging rates, respectively (CHAdeMo, n.d.-a; Electric Vehicle Charging Speeds, 2022). AC charging requires an additional on-board charger to rectify AC to DC before charging the battery, and oftentimes, the on-board charger is the limiting factor of battery charging speed. The latest fast charging technology uses DC direct charge, which removes the need for an on-board charger. Currently, there are several DC direct charging protocols: the Tesla V3 Supercharger offers up to 250 kW per car, the Combined Charging System (CCS) offers up to 350 kW, and CHAdeMO 3.0 (Chaoji) enables charging over 500 kW (The Tesla Team, 2019; CHAdeMO, n.d.-b; Berman, 2020a; SAE International, 2017). Recently, Tesla revealed the upgraded Tesla V4 Supercharger with an undisclosed specification but possibly improved over 250 kW (Kane, 2023; Lambert, 2023). Japan's CHAdeMo Association, co-developed with the China Electricity Council (CEC), on CHAdeMO 3.0 (Chaoji) should allow up to 900 kW charging rates for heavy-duty vehicles (Berman, 2020b; Edelstein, S., 2020; High Power (ChaoJi), n.d.). Germany's Charging Interface Initiative (CharIn) is developing a next-generation charging protocol called the Mega Charging System (MCS) that aims toward the trucking and transportation industries, to potentially provide up to 3.5 MW charging rates (CharIN Association, 2022; Schaal, 2022). A summary of the various charging interfaces is shown in figure 14.

A high charging capability is critical for vehicles and machinery that run on battery capacities in the range of megawatt-hours. In terms of the estimated battery capacities in

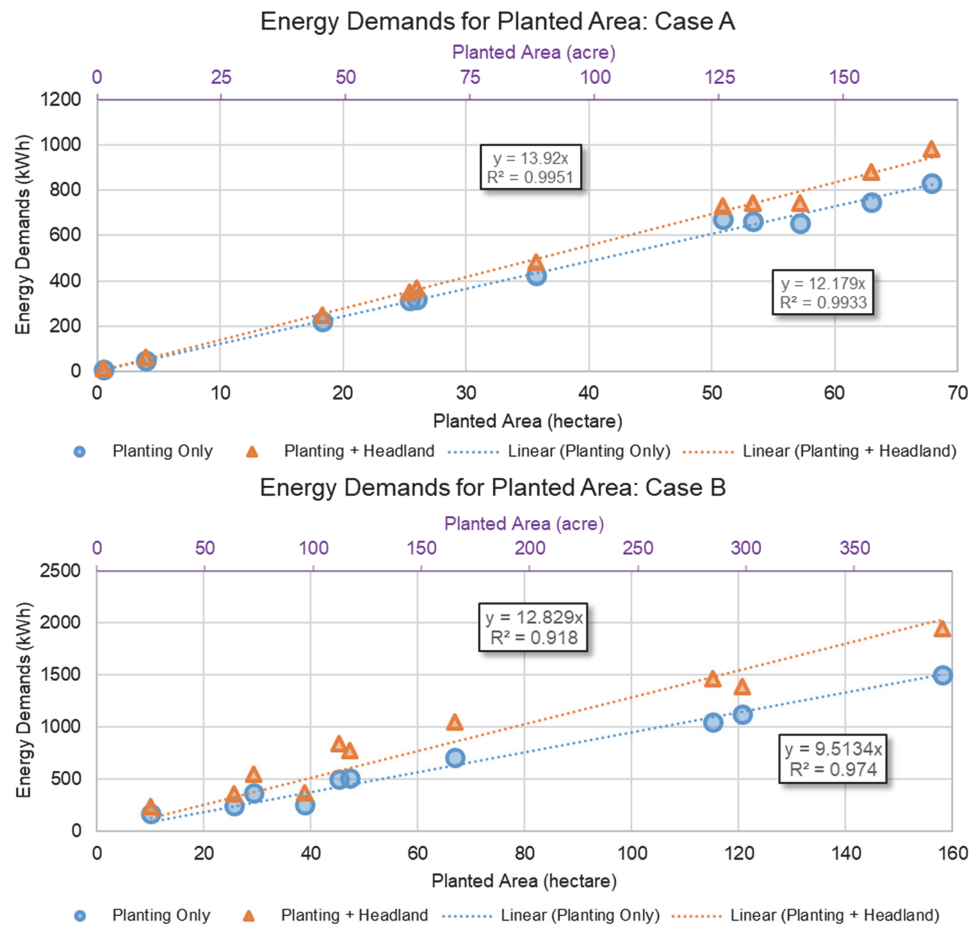

Figure 12. Energy requirement per planted area for Case A (top) and Case B (bottom). Blue labels stand for the energy demand per day while only considering the planting, whereas orange labels stand for the energy demands per day considering both planting and headland turns. For both conditions, the data were fitted with linear lines with no intercept. The R-squared scores are all above 0.9, indicating good fits.

Table 10. Energy scaling per planted area in hectare for Cases A and B.

Energy Scaler	Case A		Case B	
	kWh ha^{-1}	kWh $acre^{-1}$	kWh ha^{-1}	kWh $acre^{-1}$
Planting Only	12.2	4.9	9.5	3.9
Planting + Headland Turn	13.9	5.6	12.8	5.2

this study, given a currently available charging rate of 500 kW, Case A will still need 2.2 hours and Case B will need 5.2 hours to get a full charge.

The availability of charging stations in rural areas, as well as their proximity to farms, can be another limiting factor for the adoption of electric tractors. Currently, the majority of the charging stations for EVs are in urban or suburban regions, and there are minimal to none in most of the rural areas in the United States, which can be a major hurdle for electric tractor adoption (Tolbert, 2021).

Tractor Electrification Feasibility

The required battery size in this study was quite large. For comparison, the unballasted weights of the tractors in this study are 10,693 kg (23,574 lbs) for Case A and 19,623 kg (43,261 lbs) for Case B. The estimated battery mass would be 49.7% and 64.5% of the tractors unballasted weight for Case A and Case B, respectively. A rule of thumb for ballasting tractors is 79.1 kg per PTO kW (130 pounds per PTO horsepower) for MFWD and 66.9 kg per rated engine kW (110 pounds per rated engine horsepower) for 4WD (Tuschner, 2018). Given that Case A 7250R has a rated PTO power of 153 kW (205 hp) and Case B Xerion 5000 has a rated engine power of 386 kW (517 hp), the rules suggested a ballasted weight of 12,088 kg (26,650 lbs.) and 25,796 kg (56,870 lbs.) for Case A and B, respectively. The estimated battery mass from table 11 would still be 44.0% and 49.1% of their suggested ballasted weight, which is still very heavy. Since this study calculated battery size based on gross engine power requirements, it is likely that a large battery would be needed to account for any inefficiencies in electric motors and electric power transfer on the machine. Also, note that while the battery, inverter, and other electric power accessories will displace the traditional internal combustion engine and fuel tank, the exchange is not equivalent.

Table 11. Estimated battery sizes (volume and mass) for a full day operation without recharging.

Battery Type	Case A Battery				Case B Battery			
	Energy Capacity	Volume	Cube Length	Mass	Energy Capacity	Volume	Cube Length	Mass
Tesla Model S 18650 battery modules	1,117 kWh	3.33 m^3	1.49 m	5,319 kg	2,658 kWh	7.93 m^3	1.99 m	12,657 kg

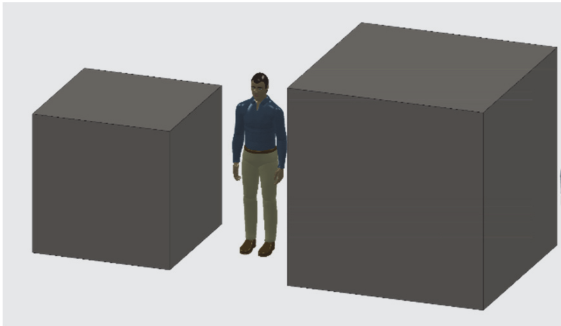

Figure 13. Comparison of battery sizes of Case A (left) and Case B (right) next to a 1.8m (6 feet) tall person as reference.

On the other hand, by allowing a recharge at midday, it is possible to cut the battery size in half. As shown in table 12, the battery sizes were cut in half and reduced to 2,660 kg (5,864 lbs.) and 6,329 kg (13,953 lbs.) and will still be able to plant about 34 hectares (84 acres) and 79 hectares (196 acres) in one full charge for Cases A and B, respectively. This will reduce the weight ratio of the battery to the ballasted weight of the tractors down to 22.0% for Case A and 24.5% for Case B. On the flip side, there will be a need for a powerful charger that can charge up the batteries within a short amount of time. The current 500kW charger will still need 1.1 hours and 2.6 hours to fully charge Case A's and Case B's batteries. The required charging time will reduce the total hectares covered per day, thereby negatively impacting the operation's field capacity.

In this study, given the tractor and planter size, the estimated battery sizes are still seemingly unrealistic; however, it is possible to design an all-electric row-crop tractor that can pull a planter with lesser row units. For example, using the ASABE estimation data from table 7, assuming 6.5 kW row^{-1} to plant at 8 km h^{-1}. It is possible for a 104-kWh battery to sustain 4 hours continuous planting for a 26-kW (35-hp) tractor and a four-row unit planter. The battery volume and mass will be 0.31 m^3 and 495 kg, and the battery can be fully charged using a 500 kW charger in under 13 minutes.

While it is still not feasible for a fully battery-powered large row-crop tractor at the current battery energy density, the battery density has been improving over time. On the cell level, the lithium-Ion battery energy density has improved from 200 Wh L^{-1} to over 700 Wh L^{-1} (3.5 times) and 80 Wh kg^{-1} to over 250 Wh kg^{-1} (3.1 times) from 1991 through 2018 (over 27 years) (Ziegler and Trancik, 2021; Crabtree et al., 2015). On the pack level, lithium-ion battery pack volumetric density has improved almost ninefold from 55 Wh L^{-1} to 450 Wh L^{-1} over the time span from 2008 to 2020 (over 12 years) (Muralidharan et al., 2022). Given the technological advancements, the battery density will improve to the point where the resulting battery size will be reasonable and a large electric row-crop tractor will be plausible.

CONCLUSIONS

This study explored two methods for determining the power requirements for row-crop planting: estimates from ASAE EP496.3 and D497.7, and calculated values from CAN-reported data. The ASABE prediction provides a good estimation of the actual planting power demands, but the planting power alone cannot account for the actual energy expenditure of tractors in the field operations. The ASABE prediction also does not contain information for hydraulic and electric power demands during planting, whose impact on actual power usage needs further investigation. CAN-reported data can be a valuable method to identify and categorize tractor operation modes. Tractor engine power was computed from the CAN-reported engine torque and engine

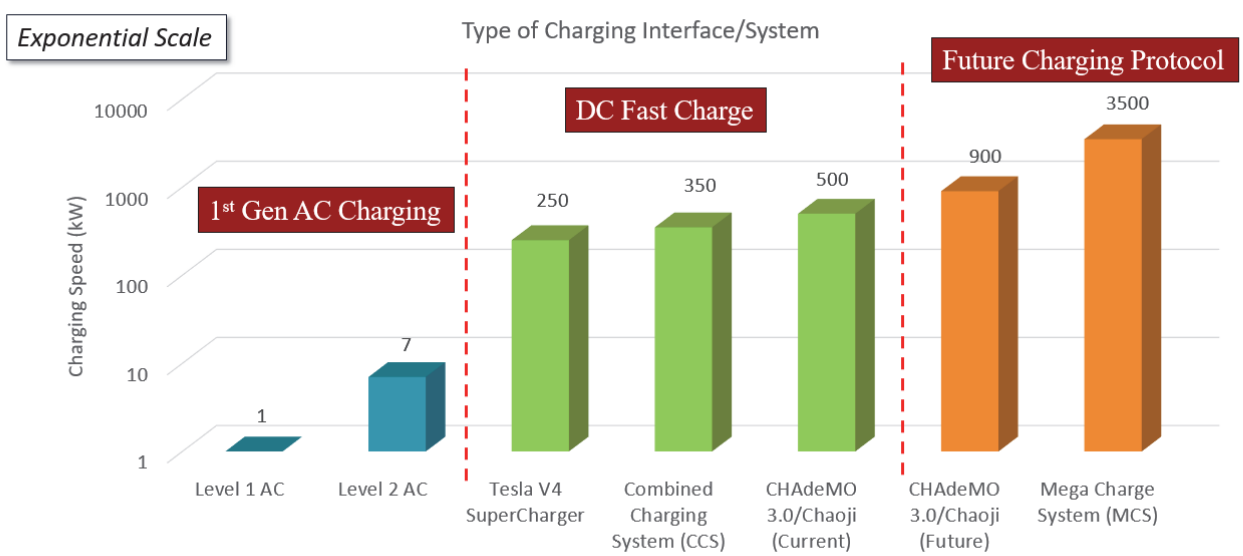

Figure 14. Existing and future electric vehicle charging systems and their rated charging speeds.

Table 12. Estimated battery mass and volume assuming a mid-day recharge is available.

	Case A Battery				Case B Battery			
Battery Type	Energy Capacity	Volume	Cube Length	Mass	Energy Capacity	Volume	Cube Length	Mass
Tesla Model S 18650 battery modules	559 kWh	1.67 m^3	1.19 m	2,660 kg	1,329 kWh	3.97 m^3	1.58 m	6,329 kg

RPM. The energy demands for the planting operation were determined from the integration of engine power over time, expressed in kWh. The daily worst-case scenarios were used for estimating the energy requirement for a fully electric row-crop tractor, which were 1,117 kWh for planting 68 hectares (168 acres) for Case A and 2,658 kWh for planting 158 hectares (391 acres) for Case B, assuming using the battery in one full charge without recharging. The daily energy demands showed a linear correlation with the daily planted area, which has energy scalars of 13.9 kWh ha^{-1} for Case A and 12.8 kWh ha^{-1} for Case B, excluding energy demands from transport and stoppage. The estimated battery mass and volume needed for a fully electric tractor are deemed unfeasible for tractor sizes and energy demands in large row-crop operations.

Acknowledgments

Thanks to the USDA AFRI Competitive Grant (Grant No. 2018-67021-27624) for sponsoring the data collection and instrumentation aspects of this project. Thanks to our collaborators Kerry Knuth, Dr. Roger Hoy, Dr. Rodney Rohrer, Nebraska Tractor Test Lab (NTTL), and Dr. Joe Luck, Keena Crone, Tyler Frederick, Tyler Smith, Hayden Sabatka, and the Eastern Nebraska Research Education Extension Center (ENREEC) for their help in collecting planting data and providing us with valuable knowledge and insights.

References

AFDC. (n.d.). Developing infrastructure to charge electric vehicles. U.S. Department of Energy, Energy Efficiency and Renewable Energy, Alternative Fuels Data Center. Retrieved from https://afdc.energy.gov/fuels/electricity_infrastructure.html

ASABE Standards. (2020a). D497.7: Agricultural machinery management data. St. Joseph, MI: ASABE.

ASABE Standards. (2020b). EP496.3: Agricultural machinery management. St. Joseph, MI: ASABE.

Berman, B. (2020a). CHAdeMO and China release new EV quick-charging standard, in a bid to leapfrog the industry. Retrieved from https://electrek.co/2020/04/28/chademo-and-china-release-new-ev-quick-charging-standard-in-a-bid-to-leapfrog-the-industry/

Berman, B. (2020b). New CHAdeMO 3.0 aims to harmonize global EV quick-charging standards. Retrieved from https://www.sae.org/news/2020/05/chademo-3.0-to-harmonize-global-ev-quick-charging-standards

Bhowmick, S. (2021). Tesla Model S battery system: An engineer's perspective. Circuit Digest. Retrieved from https://circuitdigest.com/article/tesla-model-s-battery-system-an-engineers-perspective

Brenna, M., Foiadelli, F., Leone, C., Longo, M., & Zaninelli, D. (2018). Feasibility proposal for heavy duty farm tractor. *Proc. 2018 Int. Conf. of Electrical and Electronic Technologies for Automotive* (pp. 1-6). IEEE. https://doi.org/10.23919/EETA.2018.8493236

Caterpillar. (2022). Caterpillar successfully demonstrates first battery electric large mining truck and invests in sustainable proving ground. Retrieved from https://www.caterpillar.com/en/news/corporate-press-releases/h/caterpillar-succesfully-demonstrates-first-battery-electric-large-mining-truck.html

CHAdeMo. (n.d.-a). High Power (ChaoJi). CHAdeMo. Retrieved from https://www.chademo.com/technology/high-power

CHAdeMo. (n.d.-b). Overview of CHAdeMO protocol versions. CHAdeMO. Retrieved from https://www.chademo.com/technology/protocol-development

CharIN Association. (2022). *CharIN whitepaper Megawatt Charging System (MCS).* Berlin: CharIN Association. Retrieved from https://www.charin.global/media/pages/technology/knowledge-base/c708ba3361-1670238823/whitepaper_megawatt_charging_system_1.0.pdf

Claassen, R. (2019). No-till and strip-till are widely adopted but often used in rotation with other tillage practices. US Department of Agriculture, Economic Research Service. Retrieved from https://www.ers.usda.gov/amber-waves/2019/march/no-till-and-strip-till-are-widely-adopted-but-often-used-in-rotation-with-other-tillage-practices/

Claassen, R., Bowman, M., McFadden, J., Smith, D., & Wallander, S. (2018). Tillage intensity and conservation cropping in the United States, EIB-197. US Department of Agriculture, Economic Research Service. Retrieved from https://www.ers.usda.gov/webdocs/publications/90201/eib-197.pdf?v=4171.2

CNH Industrial. (2022). CNH Industrial presents first electric tractor prototype with autonomous features. CNH Industrial Newsroom. Retrieved from https://media.cnhindustrial.com/NORTH-AMERICA/CNH-INDUSTRIAL-CORPORATE/ALL/cnh-industrial-presents-first-electric-tractor-prototype-with-autonomous-features/s/2ccdb427-427f-44bd-809c-0548d5db51c5

Crabtree, G., Kócs, E., & Trahey, L. (2015). The energy-storage frontier: Lithium-ion batteries and beyond. *MRS Bull., 40*, 1067–1078. https://doi.org/10.1557/mrs.2015.259

Cupera, J., & Sedlak, P. (2011). The use of CAN-bus messages of an agricultural tractor for monitoring its operation. *Res. Agric. Eng., 57*(4), 117-127. https://doi.org/10.17221/20/2011-RAE

Edelstein, S. (2020). CHAdeMO 3.0 fast charging for EV revealed, might be backward-compatible with CCS. Green Car Reports. Retrieved from https://www.greencarreports.com/news/1128000_chademo-3-0-fast-charging-for-evs-revealed-might-be-backward-compatible-with-ccs

Firestone. (n.d.-a). RADIAL ALL TRACTION™ DT Tire 420/90R30 (145A8). Retrieved from https://commercial.firestone.com/en-us/product/firestone/agriculture/rad-at-dt

Firestone. (n.d.-b). RADIAL ALL TRACTION™ DT Tire 710/70R42 (168A8). Retrieved from https://commercial.firestone.com/en-us/product/firestone/agriculture/rad-at-dt

Firestone. (n.d.-c). RADIAL DEEP TREAD 23° Tire 480/80R46 (158A8). Retrieved from https://commercial.firestone.com/en-us/product/firestone/agriculture/rad-dt-23

Gaetjens, B. (2022). Volvo CE upgrades electric wheel loaders. Retrieved from https://www.recyclingtoday.com/news/wheel-loader-electric-upgrade-l20-l25-fast-comfort/

Hart, A. (2022). Caterpillar tests massive battery electric mining truck destined for Australian mine. The Driven. Retrieved from https://thedriven.io/2022/11/24/caterpillar-tests-massive-battery-electric-mining-truck-destined-for-australian-mine/

Horowitz, J., Ebel, R., & Ueda, K. (2010). "No-till" farming is a growing practice, EIB-70. US Department of Agriculture, Economic Research Service. https://doi.org/10.22004/ag.econ.96636

Kane, M. (2023). Tesla's first V4 supercharger Is now open for non-Tesla EVs. InsideEVs. Retrieved from https://insideevs.com/news/661540/tesla-first-v4-supercharger-open-nontesla-evs/

Kortenbruck, D., Griepentrog, H. W., & Paraforos, D. S. (2017). Machine operation profiles generated from ISO 11783 communication data. *Comput. Electron. Agric., 140*, 227-236. https://doi.org/10.1016/j.compag.2017.05.039

Kubota Corporation. (2022). Compact electric tractor LXe-261 released in European markets. Kubota. Retrieved from https://www.kubota.com/news/2022/20220905.html

Lambert, F. (2023). Tesla Supercharger V4 revealed to be twice as powerful. Electrek. Retrieved from https://electrek.co/2023/03/15/tesla-supercharger-v4-revealed-twice-as-powerful/

Marx, S. E. (2015). Controller Area Network (CAN) Bus J1939 data acquisition methods and parameter accuracy assessment using Nebraska Tractor Test Laboratory data. MS thesis. Lincoln, NE: University of Nebraska-Lincoln, Department of Biological System Engineering. Retrieved from https://digitalcommons.unl.edu/cgi/viewcontent.cgi?article=1051&context=biosysengdiss

Marx, S. E., Luck, J. D., Hoy, R. M., Pilta, S. K., Darr, M. J., & Blankenship, E. (2015). Validation of machine CAN Bus J1939 fuel rate accuracy using Nebraska Tractor Test Laboratory fuel rate data. *Comput. Electron. Agric., 118*, 179-185. https://doi.org/10.1016/j.compag.2015.08.032

Monarch Tractor. (n.d.). Monarch Tractor Electric Tractor. Retrieved from https://www.monarchtractor.com/

Muralidharan, N., Self, E. C., Dixit, M., Du, Z., Essehli, R., Amin, R.,... Belharouak, I. (2022). Next-generation cobalt-free cathodes – a prospective solution to the battery industry’s cobalt problem. *Adv. Energy Mater., 12*(9). https://doi.org/10.1002/aenm.202103050

Nebraska Tractor Test Lab. (2014). Test 2085: John Deere 7250R. Lincoln, NE: University of Nebraska-Lincoln, Nebraska Tractor Test Lab. Retrieved from https://digitalcommons.unl.edu/tractormuseumlit/2524/

Nebraska Tractor Test Lab. (2017). Tractor Test 2175: Claas Xerion 5000 CVT. Lincoln, NE: Nebraska Tractor Test Lab, University of Nebraska-Lincoln. Retrieved from https://digitalcommons.unl.edu/tractormuseumlit/2287

NHK World-Japan. (2023). Construction equipment firm Komatsu prepares for electric launch. Retrieved from https://www3.nhk.or.jp/nhkworld/en/news/ataglance/2369/

Pitla, S. K., Lin, N., Shearer, S. A., & Luck, J. D. (2014). Use of Controller Area Network (CAN) data to determine field efficiencies of agricultural machinery. *Appl. Eng. Agric., 30*(6), 829-839. https://doi.org/10.13031/aea.30.10618

Pitla, S. K., Luck, J. D., Werner, J., Lin, N., & Shearer, S. A. (2016). In-field fuel use and load states of agricultural field machinery. *Comput. Electron. Agric., 121*, 290-300. https://doi.org/10.1016/j.compag.2015.12.023

Rohrer, R. (2017). Investigation of petroleum use in off-road agricultural machinery and analysis of J1939 Controller Area Network (CAN) data for advanced machinery testing. MS thesis. Lincoln, NE: University of Nebraska-Lincoln, Department of Biological System Engineering. Retrieved from https://digitalcommons.unl.edu/biosysengdiss/69/

Rohrer, R. A., Luck, J. D., Pitla, S. K., & Hoy, R. M. (2018). Evaluation of the accuracy of machine reported CAN data for engine torque and speed. *Trans. ASABE, 61*(5), 1547-1557. http://doi.org/10.13031/trans.12754

Rosenberg, A. B., & Wallander, S. (2022). Adoption of conservation tillage has increased over the past two decades on acreage planted to major U.S. cash crops. US Department of Agriculture, Economic Research Service. Retrieved from https://www.ers.usda.gov/data-products/chart-gallery/gallery/chart-detail/?chartId=105042

SAE International. (2017). J1772: SAE electric vehicle and plug in hybrid electric vehicle conductive charge coupler. Warrerndale, PA: SAE International. Retrieved from https://www.sae.org/standards/content/j1772/

SAE International. (2022). J1939/71: Vehicle application layer. Warrendale, PA: SAE International. Retrieved from https://www.sae.org/standards/content/j1939/71_202208/

Schaal, S. (2022). CharIN shows MW charging system commercial EVs. Electrive. Retrieved from https://www.electrive.com/2022/06/14/charin-shows-megawatt-charging-system-for-heavy-evs/

Sensiba, J. (2022). Moog & Komatsu to demonstrate fully electric wheel loader later this month. CleanTechnica. Retrieved from https://cleantechnica.com/2022/10/13/moog-komatsu-to-demonstrate-fully-electric-wheel-loader-later-this-month/

Shelton, D. P., & Rider, A. R. (2014). CC277 Energy management in field operations. *3107*. Lincoln, NE: Historical Materials from University of Nebraska-Lincoln Extension. Retrieved from http://digitalcommons.unl.edu/extensionhist/3107

Solectrac. (n.d.). The best electric tractor manufacturers | Electric tractor vs. diesel tractor. Solectrac. Retrieved from https://www.solectrac.com

The Tesla Team. (2019). Introducing V3 Supercharging. Tesla. Retrieved from https://www.tesla.com/blog/introducing-v3-supercharging

Tolbert, J. (2021). Beyond cities: Breaking through barriers to rural electric vehicle adoption. Environmental and Energy Study Institute. Retrieved from https://www.eesi.org/articles/view/beyond-cities-breaking-through-barriers-to-rural-electric-vehicle-adoption

Tuschner, J. (2018). Proper tractor ballast: Manufacturer’s answer. Ag Tire Talk. Retrieved from https://agtiretalk.com/proper-tractor-ballast-manufacturers-answer/

USDA. (n.d.). Northwest no-till farming for climate resilience. US Department of Agriculture. Retrieved from https://www.climatehubs.usda.gov/hubs/northwest/topic/northwest-no-till-farming-climate-resilience

USDOT. (2022). Electric vehicle charging speeds. US Department of Transportation. Retrieved from https://www.transportation.gov/rural/ev/toolkit/ev-basics/charging-speeds

Van Erkelens, J. (2022). VIDEO | John Deere shows autonomous electric tractor. Future Farming. Retrieved from https://www.futurefarming.com/tech-in-focus/autonomous-semi-autosteering-systems/video-john-deere-shows-autonomous-electric-tractor/

Van Hattum, B. (2019). John Deere releases video of GridCON electric tractor. Future Farming. Retrieved from https://www.futurefarming.com/tech-in-focus/john-deere-releases-video-of-gridcon-electric-tractor/

Ziegler, M. S., & Trancik, J. E. (2021). Re-examining rates of lithium-ion battery technology improvement and cost decline. *Energy Environ. Sci., 14*(4), 1635-1651. https://doi.org/10.1039/D0EE02681F